Generation of a Radial-Like Glial Cell Line

David R. Friedlander,[1] Perry A. Brittis,* Takeshi Sakurai,[1] Bronya Shif,[1] William Wirchansky,[1] Gord Fishell,[2,3] Martin Grumet[1]

[1]Department of Pharmacology, NYU Medical Center, 550 First Avenue, New York, New York 10016

[2]Department of Cell Biology, NYU Medical Center, 550 First Avenue, New York, New York 10016

[3]Skirball Developmental Genetics Program, NYU Medical Center, 550 First Avenue, New York, New York 10016

ABSTRACT: Rat C6 glioma is a cell line that has been used extensively as a model of astroglia. Although this cell line retains many of the properties of developing glia, it does not resemble morphologically the specialized form of glia found embryonically, the radial glia. In experiments designed to study a mutant form of receptor protein tyrosine phosphatase β, we isolated a subclone of C6 called C6-R which, like radial glia, assumes a highly polarized radial-like morphology in culture. C6-R cells and, to a somewhat lesser extent, C6 cells, express cytoskeletal proteins found in developing astroglia including glial fibrillary acidic protein and RC1. As seen with radial glia, cerebellar granule cell bodies and neurites migrated along radial processes of C6-R cells in culture. Morphological analysis of dye-labeled cells injected into the developing forebrain revealed that a large fraction ($\sim$60%) of the C6-R cells in the cortex assumed a radial orientation and about half of these ($\sim$30%) made contact with the pial surface. In contrast, the parental C6 cells generally formed aggregates and only displayed a radial alignment when associated with blood vessels. These results suggest that we have generated a stable cell line from C6 glioma which has adopted certain key features of radial glia, including the ability to promote neuronal migration in culture and integrate radially *in vivo* in response to local cues. This cell line may be particularly useful for studying receptors on radial glia that mediate neuronal migration. © 1998 John Wiley & Sons, Inc. J Neurobiol 37: 291–304, 1998

Keywords: radial glia; C6 glioma; cerebellar granule cells; neuronal migration; RPTPβ

Glial cells play important roles during development as well as in the mature nervous system. The first glia to develop are the radial glial cells which serve as guides for radial migration of neural cells from proliferative zones to their postmitotic destinations (Rakic, 1990). In contrast to the adult cerebellum and retina where radial glia are found as the Bergmann glia and Müller fibers, respectively, in most regions of the central nervous system radial glia are found only transiently during development and are thought to give rise to astroglia (Culican et al., 1990; Levitt et al., 1983; Alvarez-Buylla et al., 1990; Misson et al., 1988; Gray and Sanes, 1992; Voigt, 1989). Most astroglia are born after the wave of neurogenesis has subsided, and in mammals they increase to constitute the major cell type in the mature mammalian nervous system (Jacobson, 1991).

Radial glia are found in regions of the nervous system where laminated structures develop, including the cortex, cerebellum, spinal, cord and retina (Ramón y Cajal, 1995). They appear very early when the neuroepithelium is relatively thin and persist into later developmental stages where they span considerable

distances from the ventricle to the pia. Studies of radial glia *in vivo* indicate that they serve as guides for radial migration of neurons from proliferative zones (Rakic, 1990; Hatten, 1993). Cell culture experiments have confirmed that neurons can migrate along radial glia (Edmondson and Hatten, 1987). Moreover, antibody perturbation studies indicate that the migration involves astrotactin (Fishell and Hatten, 1991; Zheng et al., 1996) from the neurons and a neuron–glia junctional protein (Anton et al., 1996). To obtain primary cells as radial glia in culture, however, it is necessary to culture them with neurons or extracts from brain (Hatten, 1985; Hunter and Hatten, 1995). This need for extrinsic factors to maintain radial glia in culture makes it difficult to study these cells in isolation. Much remains to be learned about these cells, and the availability of radial glial cell lines would make this specialized cell type amenable for the first time to molecular and biochemical analysis *in vitro*.

Studies of astroglia have benefited from investigations of brain tissue as well as the use of primary cells and cell lines in culture. Most glial cell lines have been derived from gliomas, and some have been established by immortalizing cells (McKay et al., 1990) or by clonal selection (Alliot and Pessac, 1984). Tumor cell lines retain many of the hallmarks of astroglia and have been useful models for molecular and cellular studies of many of their characteristics. While cell lines have been useful for studying various properties of astroglia, radial glial cell lines have not yet been established.

In the course of selecting C6 rat glioma cells that were transfected with a plasmid encoding a truncated receptor phosphatase (Levy et al., 1993), we obtained a clone called C6-R that exhibited remarkable radial morphology in culture. Interestingly, the majority of the C6-R cells had highly polarized morphologies following injection of labeled cells into the developing forebrain. In this article, we characterize this radial-like cell line by comparing its properties with parental C6 glioma cells. The results of this analysis suggest that we have identified an immortalized cell line with phenotypic properties of radial glia. As such, this line provides a valuable model for this elusive cell type.

MATERIALS AND METHODS

Establishment of C6-R Cell Line

C6 glioma cells were obtained from the American Type Culture Collection (Bethesda, MD) and cultured in Dulbecco's modified Eagle's medium (DMEM; Biowhittaker, Walkersville, MD)/10% fetal calf serum (FCS; Life Technologies, Gaithersburg, MD). DNA encoding the human receptor protein tyrosine phosphatase-β (RPTPβ) short form (nucleotides 1–2655, *ClaI* site at the 3′ end) in Bluescript SKII was kindly provided by Dr. G. Barnea and Dr. J. Schlessinger at the NYU Medical Center. The *ClaI* and *ApaI* (from the multicloning site) fragment of this clone was replaced with a polymerasechain reaction (PCR) fragment encoding an hemagglutinin (HA) tag followed by a stop codon in frame. Primers for PCR were 5′-GCAATCGATACGGCCGCATCTTTTA-CCC-3′ (*ClaI* site is underlined) and 5′-CGTGGGCCCTAG-CACTGAGCAGCGTAATCTG-3′ (*ApaI* site is underlined and stop codon is in bold); the PCR template was DNA encoding HA tag sequences in the *NotI* site of Bluescript SK, kindly provided by Dr. Schlessinger (Hu et al., 1993). The construct was cut by *SacI* (multicloning site), treated with Klenow fragment in the presence of four deoxynucleotide triphosphates, digested again with *ApaI*, and inserted into pCDNA3 (Invitrogen, San Diego, CA) using *EcoRV* and *ApaI*. Sequences for both strands were confirmed by sequencing. Twenty micrograms of DNA was mixed with 50 μL of lipofectin (Life Technologies) and transfected into C6 glioma cells using opti-MEM media (Life Technologies). Stable transfectants were selected with G418 (1.5 mg/mL effective concentration) and more than 50 colonies were picked from three independent transfections. Each cell line was screened by Western blotting of cell extracts using monoclonal antibody 12CA5 against the anti-HA tag (Boehringer Mannheim, Indianapolis, IN).

Cell Culture and Interactions with Neurons

C6 and its transfectants including C6-R were maintained in DMEM/10% FCS. For immunofluorescence studies, cells were plated onto 2.5-mm wells of 26-well slides (Cel-Line Associates, Newfield, NJ). Interactions with neurons were observed using either dissociated cerebellar granule cells on sparse glia or aggregates of granule cells on confluent glial monolayers. Confluent cell monolayers of C6 or C6-R cells were prepared by growing 3×10^4 cells per 4-mm well of 24-well glass slides (Cel-Line Associates) for 2–4 days. Cerebellar granule cells from P4 rats were prepared by trypsinization, fractionation on a two-step (35% and 60%) Percoll gradient (Sigma, St. Louis, MO), and preplating on tissue culture dishes coated with poly-L-polylysine (Sigma) as described (Hatten, 1985). A total of 10^5 dissociated granule cells were seeded in wells with sparse glia. Aggregates of granule cells were formed during overnight incubation with shaking (Friedlander et al., 1996), and approximately 10 aggregates of labeled cerebellar granule cells were added to each confluent monolayer. The migratory behavior of 1,1′-dioctadecyl-3,3,3′,3′-tetramethyl-indocarbocyanine perchlorate (DiI)-labeled granule cell bodies and neurites was observed under phase and fluorescence microscopy. Static and time-lapse recordings were made following overnight incubation. The patterns of the neuronal aggre-

gates on confluent glial monolayers were obtained at 1 and 27 h after introduction of the aggregates. Images were digitized using a Cohu CCD camera and a Scion image grabber, and analyzed using NIH Image software. To quantify the extent and polarity of cell body migration, the area defined by the margins of the region occupied by labeled cells, as well as the length of the major and minor axes of the associated fitted elipses, were obtained. Polarity was defined as $a/b - 1$, where a and b are the major and minor axes of the ellipse, respectively. Experimental points represented measurements made on aggregates with nonoverlapping outgrowth in four to 10 replicate wells; four independent experiments were performed.

Immunofluorescence

Cells to be stained with antibodies directed against cytoskeletal proteins were fixed with 2% paraformaldehyde for 5 min followed by treatment with methanol at 4°C for 5 min. Otherwise, they were fixed with 4% paraformaldehyde for 20 min. To detect intracellular epitopes, cells were permeabilized with 0.1% Triton X-100 for 10 min. Primary antibodies included monoclonal antibodies (mABs) rat-401 (anti-nestin hybridoma supernatant; Developmental Studies Hybridoma Bank, University of Iowa), RC1 (hybridoma supernatant; provided by Dr. A. L. Pearlman), anti-Gap-43 clone 91E12 and anti-vimentin clone V9 (1:200 and 1:4 dilutions, respectively; Boehringer Mannheim, Indianapolis, IN), and anti-neurofilament SMI 32 (1:1000; Sternberger Monoclonals). Polyclonal antibodies included anti–glial fibrillary acidic protein (GFAP) (1:200; Dako, Carpenteria, CA) and anti-brain lipid binding protein (BLBP) (provided by Dr. Nat Heintz). Secondary antibodies included lissamine rhodamine-conjugated anti-mouse immunoglobulin G (IgG), lissamine rhodamine-conjugated anti-mouse IgM, and lissamine rhodamine-conjugated anti-rabbit Ig (1:200; Jackson Immunoresearch Laboratories, West Grove, PA).

Cell Labeling

C6 and C6-R cell lines were intrinsically labeled through incubation with DiI (Molecular Probes, Eugene, OR) (Friedlander et al., 1989) or by cotransfection with the plasmid pEGFP-N1 (Clontech, Palo Alto, CA), which codes for green fluorescent protein (GFP) (Chalfie et al., 1994) and a plasmid conferring resistance to hygromycin; selection was performed using 300 μg/mL of hygromycin. Transfections were performed using Lipofectamine (Life Technologies). Cerebellar granule cells were labeled in suspension for 10 min with 30 μg/mL DiI in CGL-DIL diluent (Sigma) immediately after the Percoll-gradient procedure.

Introduction of Cell Lines into Developing Rat Brain

C6 and C6-R cells were injected into embryonic day 16 (E16) rat embryo brains as previously described (Fishell,

1995; Fishell and van der Kooy, 1987). In brief, following laparotomy, the uterine horns were exposed and embryos visualized through transillumination. Using the calvarian sutures as a landmark, 1 μL of cell suspension containing 1.5×10^7 cells/mL in Ham's F12 medium was injected through the uterine wall into the cerebral ventricles of host embryo forebrains; the use of Fast green confirmed injection into the ventricles. Approximately 70% of the injected embryos survived the procedure.

Examination of Injected Cells in Host Brain

Both embryo and pup brains were fixed in 4% paraformaldehyde–phosphate-buffered saline (PBS); embryos were decapitated and their heads fixed by overnight immersion. Pups were first perfused with 4% paraformaldehyde and then immersed in fixative overnight. To analyze cells labeled with DiI, brain slices were cut with a vibratome and visualized through fluorescence microscopy; four C6 and five C6-R embryos, and eight C6 and six C6-R pups were examined. For cells labeled with GFP, frozen brain sections were prepared using a cryostat; 24 C6 and 26 C6-R embryos were examined.

Three embryonic brains from two different experiments were serially sectioned and used for quantification of cell number and process length measurements. To evaluate cell morphology and polarization, single GFP-positive cells located within 600 μm from the pial surface of the telencephalon were selected and counted. The dorsomedial region was chosen to simplify the analysis and avoid nonradial patterns of morphology observed in other regions such as near the ventricle. To quantify cell length, the longest fluorescent profile was detected through various focal planes and measured. In addition, a subset of these cells which contacted the pial surface was counted and represented as the percentage of the total number detected. Quantitation was performed on images captured with the CCD camera using NIH Image.

Immunoblots

Confluent C6 parental and C6-R cells in 100-mm dishes were lysed in 0.5 mL of extraction buffer containing 1% Triton X-100 and cleared by centrifugation as described elsewhere (Sakurai et al., 1996). Protein concentration was determined using the Bradford method with BSA as a standard, and 50 μg of cell extracts was resolved on sodium dodecyl sulfate–polyacrylamide gel electrophoresis. Proteins were transferred to nitrocellulose membranes and blotted with the anti-HA tag mAB 12CA5 (1 μg/mL; Boehringer Mannheim), mAB anti-α-tubulin (Amersham, Arlington Heights, IL), or polyclonal anti-GFAP followed by anti-mouse or anti-rabbit Ig conjugated with horseradish peroxidase (1:5000 dilution; Amersham) and were visualized using a chemiluminescence detection kit (NEN, Boston, MA). The anti-HA mAB recognized a major 190-kD species in C6-R but not in parental C6 cell extracts. This

band, as well as a larger one (~250 kD, which is probably a proteoglycan form), was precipitated by anti-rat phosphacan as well as by anti-human RPTPβ polyclonal antibodies and was recognized by anti-HA tag antibody (data not shown), suggesting that the 190-kD species represents the mutant form of RPTPβ. Similar bands were observed in extracts from COS7 cells transiently transfected with the same construct (data not shown).

RESULTS

To analyze the function of RPTPβ (Levy et al., 1993; Maurel et al., 1994; Canoll et al., 1996; Grumet et al., 1996) in glia, we attempted to use a dominant negative paradigm. C6 glioma cells which normally express RPTPβ (Sakurai et al., 1996) were transfected with a construct encoding a mutant form of the human receptor containing an HA tag in place of the two cytoplasmic phosphatase domains. Among the cell lines that were obtained, one called C6-R assumed a highly polarized morphology in culture [Fig. 1(A)]. Several cell lines including C6-R expressed the human truncated form of RPTPβ that was detected by immunoblotting with antibodies against the HA tag [insert in Fig. 1(D)]. Many of the transformants assumed a more stellate morphology than the parental C6 cells, but the morphological changes did not correlate with the level of expression of the truncated receptor. In several additional experiments, transfection of C6 cells using the same plasmid, as well as the same region of RPTPβ in pMAMneo (inducible with dexamethasone) and in pEGFP-N1 (as a fusion protein with green fluorescent protein) and control plasmids, did not yield any clones with a stable radial-like phenotype resembling C6-R (data not shown). The combined data suggest that the radial-like morphology cannot simply be due to expression of the truncated RPTPß; however, its expression may contribute to polarization of the cell. Potential mechanisms underlying the generation of C6-R are summarized in the Discussion. The properties of C6-R compared to the parental cell line are described below.

Characterization of C6-R Cells in Culture

Several hours after attaching to tissue culture plates, C6-R cells were observed as polarized cells. The morphological phenotype of C6-R was stable after more than 10 passages. This morphology was observed even at low cell density, and conditioned medium from C6-R did not alter the morphology of parental C6 cells, indicating that this phenotype
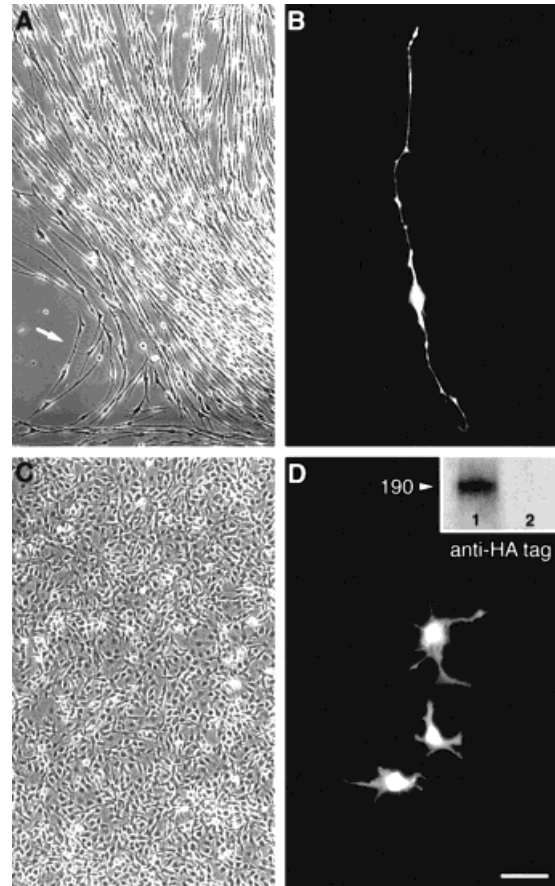

Figure 1 Morphology of C6 and C6-R glioma cells *in vitro*. Phase-contrast micrographs of cultured C6-R cells (A) and C6 glioma cells (C). Fluorescence micrographs of cultured GFP-expressing C6-R cells (B) and C6 cells (D) grown on monolayers of nonfluorescent C6 cells. Note the radial shape and orientation of the C6-R cells in culture [arrow in (A)] and how the GFP labels the entire cell (B,D). [(D), inset] Western blot analysis of C6 and C6-R probed with anti-HA tag antibodies to identify the truncated form of human RPTPβ. The HA tag was detected in the transfected C6-R cells (lane 1) but could not be detected in the parental C6 cells (lane 2). Scale bars: 150 μm in (A,C) and 40 μm in (B,D).

was unlikely to be due to secreted factors. C6-R cells proliferate in culture at a rate that is slightly slower than that of the parental cells (P. Brittis, D. Friedlander, and M. Grumet, unpublished observations). Prior to cytokinesis, C6-R cells withdrew both of their radial processes, and following cytokinesis the daughter cells usually reextended the radial process along the orientation of their parental cell. This is likely to account for the coalignment of C6-R in culture [Fig. 1(A)].

To observe the behavior of the C6-R cells in combinations with other cells in culture and *in vivo*, we
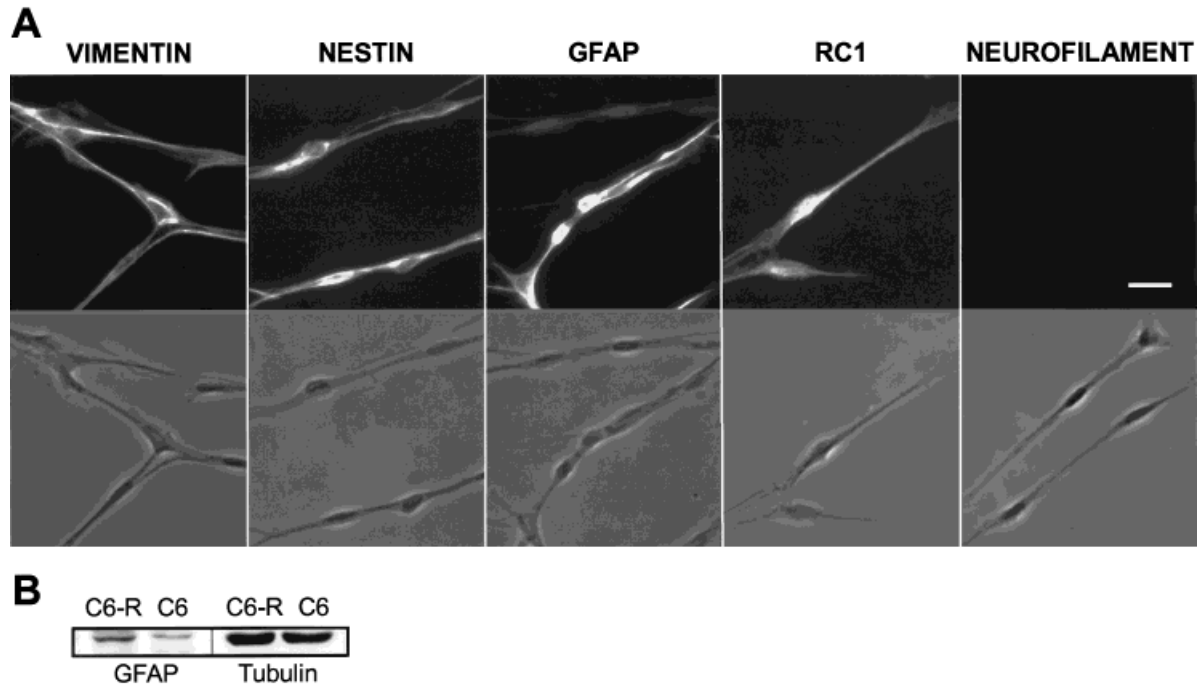
A

B

Figure 2 Expression of glial markers by C6-R cells. (A) The top row shows fluorescence images of C6-R cells stained with specific antibodies against the indicated cytoskeletal proteins, as described in Materials and Methods. Matched-phase micrographs are shown in the bottom row. Note the bright fluorescence images of C6-R cells stained for vimentin, nestin, GFAP, and RC1, in contrast to the lack of staining for neurofilaments. GFAP expression was heterogeneous within the cell population. Bar = 20 μm. (B) Immunoblot of 50 μg each of C6-R and C6 cell extracts probed with anti-GFAP (1:1000 dilution) and anti-tubulin (1:3000) antibodies.

established stable lines for C6 and C6-R expressing GFP. Individual clones of C6-R cells expressing GFP resembled the C6-R cells morphologically. When a small percentage of C6-R cells expressing GFP were cocultured to confluence with parental C6 cells (GFP negative), they maintained a highly polarized morphology [Fig. 1(B)]. In contrast, C6 glioma had a polygonal shape under similar conditions [Fig. 1(D)]. The results suggest that the morphological phenotype of C6-R in culture is cell autonomous.

Given the striking morphology of the C6-R cells, it was interesting to characterize these cells with markers for developing glial cells. Immunofluorescent staining of C6-R (Fig. 2) cells showed expression of vimentin, nestin, GFAP, and the radial glial marker RC1, cytoskeletal proteins found in different stages of developing astrocytes and radial glia (Culican et al., 1990; Edwards et al., 1990; Hockfield and McKay, 1985). These markers were also found in the parental C6 cells, but GFAP and RC1 were more prevalent in C6-R cells. In contrast to the relatively uniform staining observed for vimentin and nestin, the intensity of staining for GFAP, which is up-regulated during glial maturation, varied among cell populations. Whereas all cells stained at least weakly for

GFAP, the majority of C6-R cells (55%) stained strongly, while only a few C6 cells (9.3%) did. This difference was confirmed in immunoblots with anti-GFAP antibodies on extracts of the cells that showed stronger reaction in C6-R cells than in C6 cells. The C6-R cells did not stain with antibodies that recognize neurons including anti-neurofilament protein TUJ1 and anti-Gap43 (Fig. 2 and data not shown). In addition, very weak or no specific staining was detected with markers for oligodendrocytes including O4, Rip, myelin basic protein, and proteo-lipid protein (data not shown).

The staining with vimentin and nestin is characteristic of developing neuroepithelial cells, and the elevated levels of GFAP and RC1 in C6-R suggest astroglial or radial glial differentiation. There is no evidence for neuronal differentiation in C6-R. Another marker for radial glia in mice, anti-BLBP (Feng and Heintz, 1995), was not useful for C6-R insofar as it did not react with rat cells. In the absence of a definitive set of markers to define rat radial glia in culture, the morphology combined with the marker studies is consistent with the notion that C6-R represents radial glia.
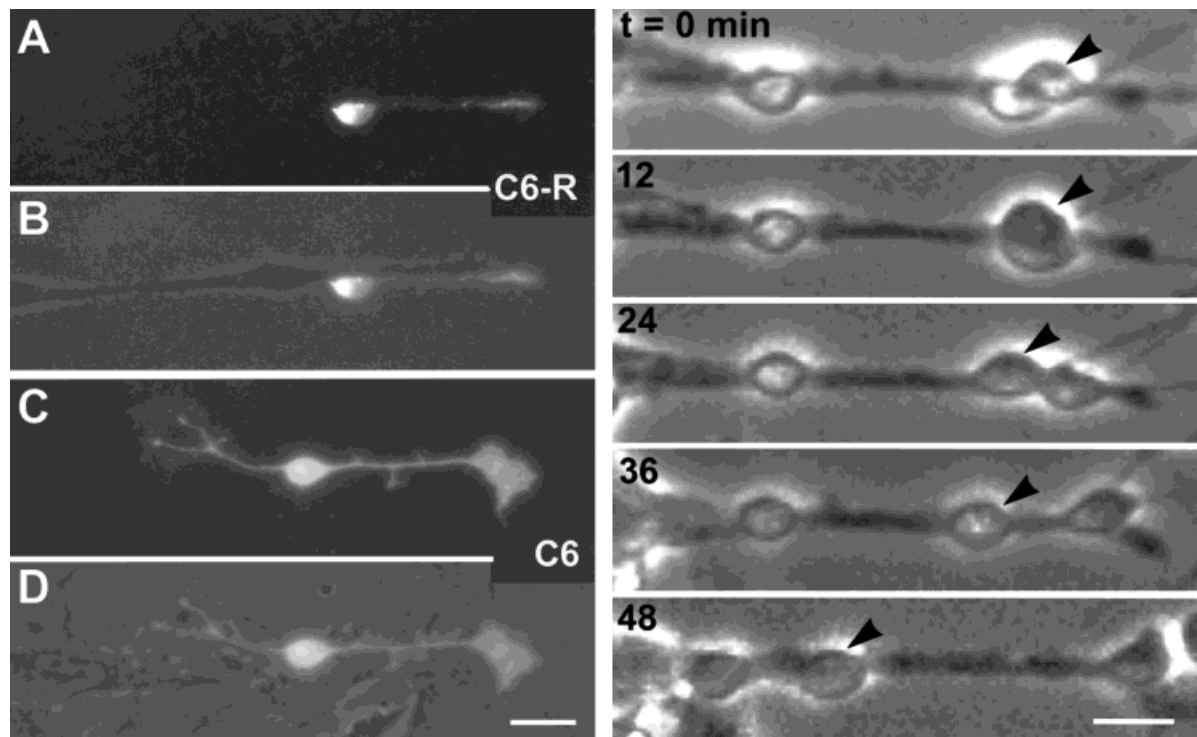
Figure 3 Morphology and migration of cerebellar granule cells on C6-R cells. Fluorescently labeled cerebellar granule cells were added to sparse cultures of C6-R cells [(A,B) and right panel] or C6 cells (C,D) and granule cell behavior was analyzed through fluorescence microscopy (A–D) and time-lapse recordings (right panel). (B,D) Superimposed phase and fluorescence images of the fields presented in (A,C), respectively. Note the close association of the granule cell process with the C6-R cell and the club-shaped end of the leading process (A,B). This is in sharp contrast to the wide growth cone, filopodia, and neuritic branches of granule cells on C6 cells (C,D). The right panel shows images from a time-lapse recording of three granule cells (phase bright) associated with a C6-R process (phase dark); the images are separated by 12-min intervals. Note the leftward migration of the granule cell marked by the arrowhead: in particular, the large displacement during the last 12-min interval (36–48 min). Note also the rightward migration of the granule cell in contact with the marked cell. Bars = 20 μm.

Cerebellar Granule Cells Migrate along C6-R Cells

Previous studies of radial glia in culture have shown that they support migration of cerebellar granule cells (Hatten, 1993). Therefore, it was interesting to test whether C6-R could support neuronal migration. Dissociated granule cells were found to adhere to sparsely distributed C6-R cells on tissue culture plates. Many of the granule cells exhibited a migrating profile with a teardrop-shaped cell body and a leading process (Edmondson and Hatten, 1987; Rivas and Hatten, 1995) on C6-R cells [Fig. 3(A,B)]. In contrast, on the parental C6 cells many granule cells had neuritic extensions, filopodia, and growth cones [Fig. 3(C,D)]. Moreover, time-lapse recordings showed saltatory movement of granule cell bodies along C6-R cells with individual neurons exhibiting

average migration speeds ranging from 0 to 70 μm/h; the average maximal speed of migration in four experiments was 63 ± 19.4 μm/h. Multiple granule cells were observed to migrate in the same direction on individual C6-R cells. Occasionally, they were found to migrate in opposite directions and passed each other on individual C6-R cells (Fig. 3). Notably, their mode of migration was highly reminiscent of the migration of granule cells on radial glia (Edmondson and Hatten, 1987). These types of movements were not seen on C6 cells, but instead, the granule cells had active growth cones. The results indicate that both the morphology and movement of granule cells differed for C6 and C6-R cells.

Given the saltatory nature of neuronal migration, we decided to use a population model to analyze neuronal migration in culture. Taking advantage of
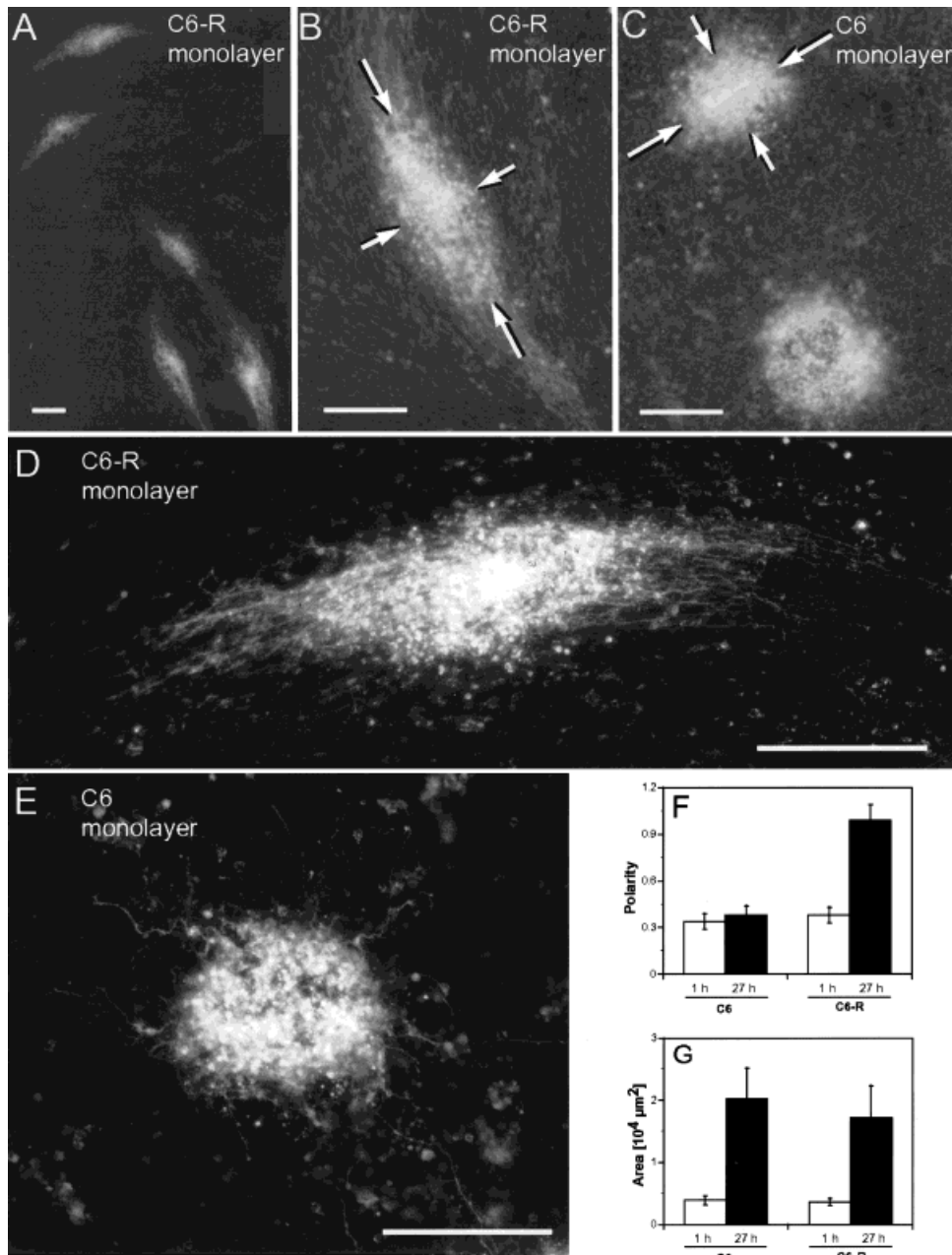
Figure 4 Migration of cerebellar granule neurons along C6-R cells. Aggregates of DiI-labeled granule cells were seeded on confluent monolayers of C6-R (A,B,D) and C6 (C,E) cells and photographed after coculture for 27 h. Long and short arrow pairs indicate major and minor axes, respectively (B,C). Note the numerous polarized granule cell processes extending on C6-R monolayers (D) in contrast to the few processes on C6 monolayers. The polarity (F) and the area (G) covered by each aggregate were determined at the times indicated. The areas of the aggregates were very similar on C6 and C6-R cells, but the shape of the granule cell collectives was more polarized on the C6-R cells (F) and was oriented along the long axis of these cells (A,B). Bars in (F,G): means of four independent experiments; error bars = standard error. Scale bars = 200 μm.

the fact that C6-R cells align with each other in culture [Fig. 1(A)], which resembles the alignment of radial glia as palisades *in vivo*, we tested whether C6-R cells could direct migration of cerebellar granule neurons in culture. When aggregates of granule neurons were seeded on confluent monolayers of C6
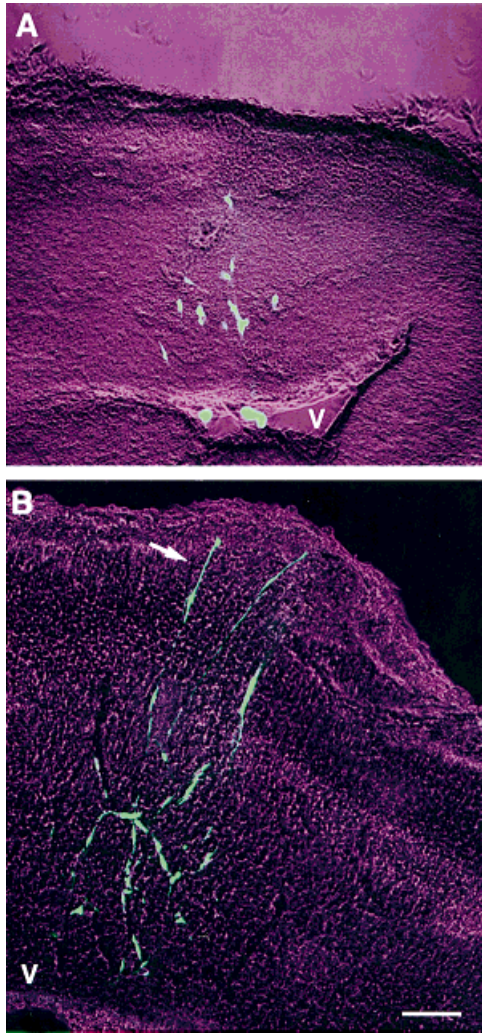
Figure 5 Mixed phase-contrast and fluorescence micrographs showing GFP-positive (green) C6 (A) and C6-R (B) cells within the E19 telencephalon. GFP-positive cells were injected into the ventricle (V) at E16 and the embryos were sacrificed after 3 days. Note in (B) how the C6-R cells extend long radial processes toward the pial surface (arrow). Scale bar = 200 μm.

cells, the neurons and their processes migrated in a random pattern away from the aggregates (Fig. 4). In striking contrast to this isotropic migration, granule cells migrated preferentially along the radial processes of C6-R cells with a subpopulation of neurons migrating more extensively on C6-R than on C6 [Fig. 4(A–C)]. Moreover, neuritic processes extending from the granule cells were also oriented along the radial processes of C6-R and extended further than neurites on C6 cells [Fig. 4(D,E)]. The pattern of neuronal cell bodies on C6-R monolayers resembled an ellipse; we therefore measured the long and short axes of the aggregates to calculate the polarity [Fig.

4(B)]. Whereas there was little or no change in the polarity of the neuronal aggregates on C6 cells, there was a dramatic increase on monolayers of C6-R cells [Fig. 4(F)]. In contrast, the area covered by the neuronal aggregates on C6 and C6-R cells did not differ significantly [Fig. 4(G)]. The combined results indicate that granule cell neurons migrate preferentially along the radial axis of C6-R cells.

Characterization of C6-R Cells *In Vivo*

Given their glial lineage, these results suggest that C6-R cells have adopted some critical characteristics of radial glial cells. To more stringently test this possibility, we investigated the phenotype of the C6-R cells by comparison with parental C6 cells, following injection of dye-labeled cells into the developing forebrain. Fluorescently labeled cells were injected into rat forebrains at ~E16 and cells were subsequently analyzed in sections of brains from embryos or postnatal rats by fluorescence microscopy. Initial experiments performed using DiI to label cell membranes showed the presence of fluorescent cells 3–20 days after injection. In contrast to the C6 cells which had polygonal shapes and tended to form aggregates, C6-R cells were often found as highly polarized cells oriented along the radial axis of the neuroepithelium (Fig. 5; see also Fig. 7). The results indicated that the majority of C6-R cells could integrate into the embryonic rat brain and responded to local cues to become oriented in a radial-like morphology aligned
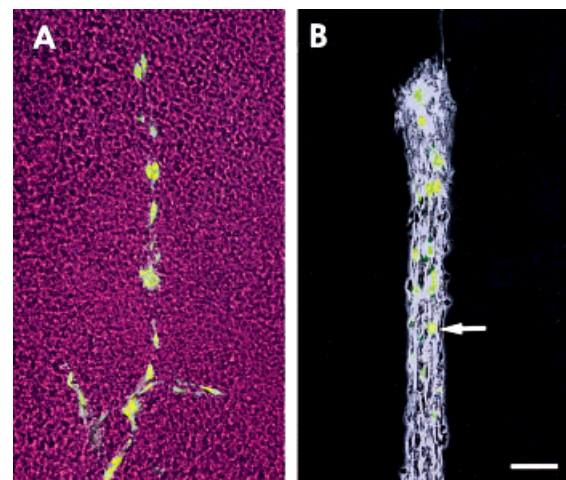

Figure 6 C6 glioma cell migration over blood vessels. (A) Phase-contrast micrograph of GFP-positive cells (green) aligned on a presumptive blood vessel in a E19 embryo. (B) GFP-positive C6 glioma cells (green; see arrow) on a blood vessel which had been teased out of a P10 brain. Scale bar = 50 μm.

with radial glia *in vivo*. Some C6-R cells apparently did not penetrate very far into the cortex and remained near the ventricle with less polarized morphologies.

While DiI is a very useful marker for membranes, an expressed marker protein is advantageous insofar as it does not become diluted as cells divide and it allows one to rule out the possibility of dye transfer from plasma membranes of implanted cells to the host. Thus, to investigate further the behavior of the C6-R cells by comparison with the parental C6 cells in greater detail, we decided to use GFP-expressing cell lines given that GFP is expressed inside the cell. Analysis of GFP-labeled cells in embryonic telencephalon revealed patterns identical to those seen with the DiI label. Three days following injection, C6 cells were found as polygonal cells, while many of the C6-R cells were highly polarized, often being aligned along the radial axis of the tissue (Fig. 5). Radial organization of C6 cells was observed only when they were aligned along blood vessels. Both C6 and C6-R appeared to associate with blood vessels in embryonic brain [Fig. 6(A)], and fluorescently labeled cells were found on vessels after they were dissected from postnatal brain [Fig. 6(B)].

Observations of cells at higher magnification showed that C6 occasionally had processes, but they were not as long as those generally seen with C6-R cells (Figs. 7 and 8). Moreover, C6-R cells were often aligned with the radial glia [Fig. 7(D)] and perpendicular to the ventricular surface [Fig. 7(B, D–F)]. In contrast, the orientation of the C6 cells appeared to be random [Fig. 7(A)]. Furthermore, C6 were often found as aggregates [Fig. 7(C)].

By postembryonic day 10 (P10), radial glia within the cortex largely disappear and are thought to transform into astrocytes (Voigt, 1989). While the majority of our studies were performed on embryos 3 days following injection of cells, in a few cases, litters were born and fluorescently labeled C6-R radial cells were also found in P10 brains. The alignment and morphology of some of the C6-R cells were strikingly similar to those of the radial glia. Processes of C6-R cells closely followed the orientation of the native radial glia over large distances [Fig. 7(F)], and many C6-R cells extended processes toward the ventricular surface. In addition, some fluorescent C6-R cells in P10 brains exhibited stellate morphologies resembling more mature glia [insert in Fig. 7(F)] which are known to develop at later stages.

To quantitatively compare the morphologies of C6 with C6-R following implantation in embryonic rat telencephalon, we measured two parameters: the number of cells reaching the pial surface and the length of the cells (Fig. 8). A large proportion of the C6-R cells (~30%) were found to reach the pial surface, but a much smaller proportion of C6 cells (~3%) were detected at the pia [Fig. 8(C)]. Given that the cells in both groups were injected into the ventricle, these results suggest that the C6-R cells can migrate within the brain more extensively than C6 cells. The length distribution of C6-R and C6 differed dramatically and had minimal overlap, with the longest C6-R cells being ~300 μm in length [Fig. 8(D)]. The median length of C6-R cells was 131.5 ± 11.5 μm, which was significantly longer than the 42.4 ± 2.2 μm observed for the C6 cells. Approximately 60% of the C6-R cells *in vivo* were longer than 100 μm and were highly polarized [Fig. 8(D)].

DISCUSSION

We generated a variant of the rat C6 glioma cell line, C6-R, that has a highly polarized morphology in culture and *in vivo* following injection into the developing nervous system. Cytoskeletal proteins found in C6-R are characteristic for developing astroglia and radial glia but not for other neural cells. C6-R cells align with their neighbors in culture. They also integrate and differentiate with morphologies that resemble radial glia *in vivo*. In addition, cerebellar granule neurons migrate preferentially along the radial axis of C6-R in culture. Thus, the C6-R cell line has two key similarities to radial glial cells that make it useful as a model for these cells: (a) its morphology and (b) its ability to support neuronal migration. Given that radial glia are difficult to purify and obtain in sufficiently large amounts for biochemical analysis, radial glial cell lines provide unique opportunities for cellular and biochemical analyses.

Factors that control development and differentiation of radial glia have been difficult to study. Cerebellar radial glia can be obtained in culture when they are cocultured with granule cell neurons (Hatten, 1985). Recent studies indicate that radial glial transformation to astrocytes is bidirectional and can be controlled by a diffusible factor in embryonic brain (Hunter and Hatten, 1995). Moreover, Cajal-Retzius cells can regulate the radial glia phenotype in developing and adult cerebellum by diffusible signals (Soriano et al., 1997). If the C6-R cells represent a glial cell trapped in a radial phenotype, molecular approaches to find differences between C6 and C6-R such as differential display (Liang and Pardee, 1992) and suppression subtractive hybridization (Diatchenko et al., 1996) may be useful in identifying and purifying proteins that regulate the radial glial phenotype.
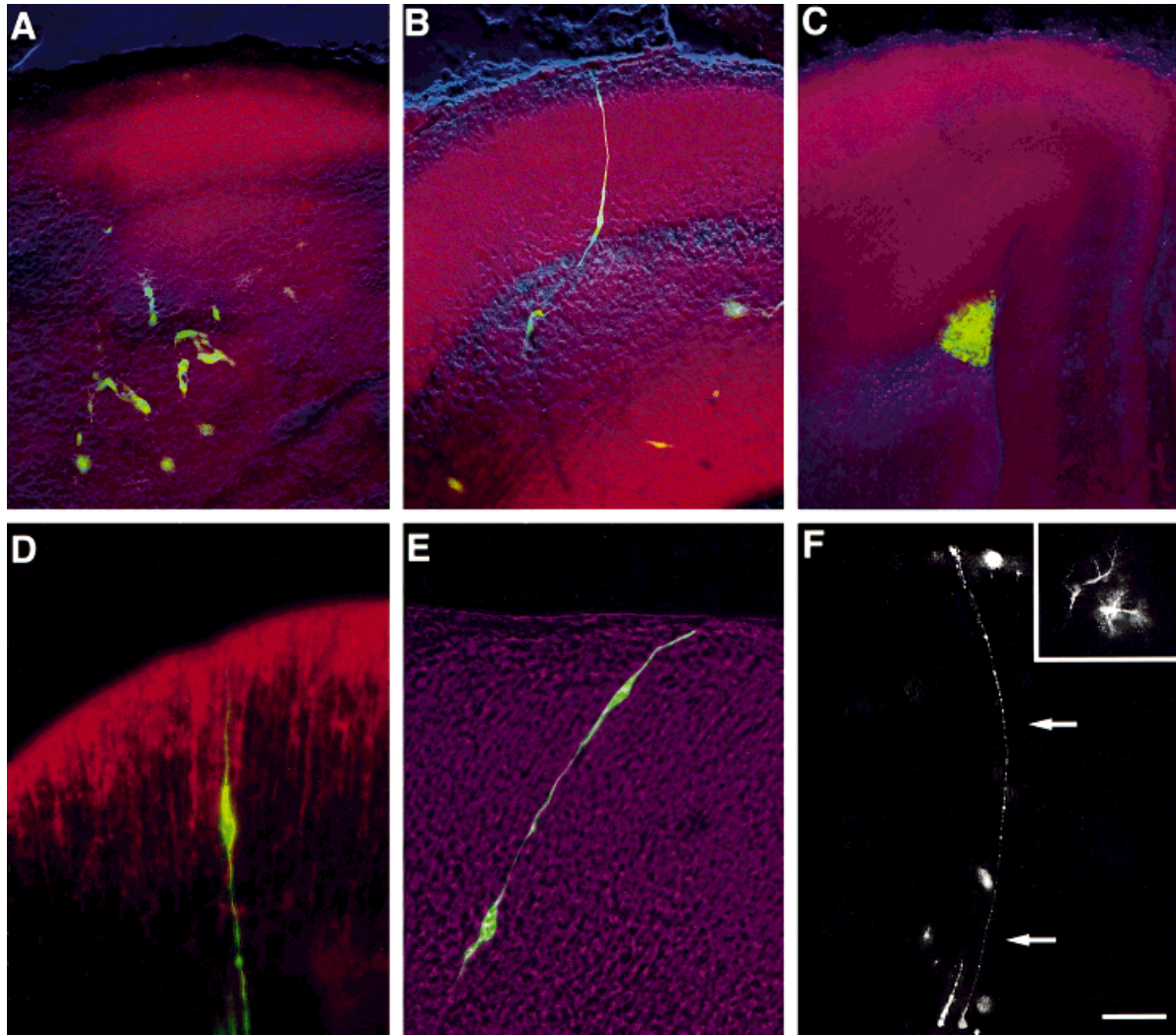
Figure 7 Visualization of GFP-positive C6 and C6-R cells following injections at E16. (A–C) Sections were counterstained with propidium iodide (red) and viewed using Nomarski optics (blue). (A) Embryo injected with GFP-positive C6 cells harvested at E19. In these animals, the majority of the cells had a simple morphology and did not extend processes toward the pial surface. (B) At E19, C6-R cells had a radial morphology with long processes that were anchored to the pial surface by end feet and extended toward the ventricular surface. (C) GFP-positive C6 cells as a cluster near the ventricular angle formed by the apposition of the striatum and the cortex in an E19 embryo. (D) A GFP-positive C6-R cell (green) coaligned with anti-nestin–labeled (red) radial cells in the cortex. (E) GFP-positive C6-R cells (green) located within the E19 cortex. (F) DiI-labeled C6-R cells were injected at E16 and visualized in animals sacrificed 15 days postinjection. Many of these cells maintained a long process (arrows) which was anchored to the pial surface. The insert in (F) shows DiI labeled C6-R cells 15 days postinjection with stellate morphologies located near the pial surface. Scale bars: 50 μm in (A–C), 30 μm in (D,E), and 200 μm in (F).

Although the phenotype of C6-R in culture is very stable, these cells appear to respond to some local cues. As many as 60% of C6-R cells take on a highly polarized radial-like appearance in the cortex. Remarkably, many of the radial-like C6-R cells migrate into the cortex and align with the endogenous radial glia, and 30% of these cells appear to reach the pial surface. In addition, in a few animals that were maintained for several weeks before analysis, one could find labeled cells that had morphologies resembling mature astrocytes, suggesting that some C6-R cells may differentiate along this pathway *in vivo*. Additional studies are needed to determine whether the proportion of the stellate cells increases with time.
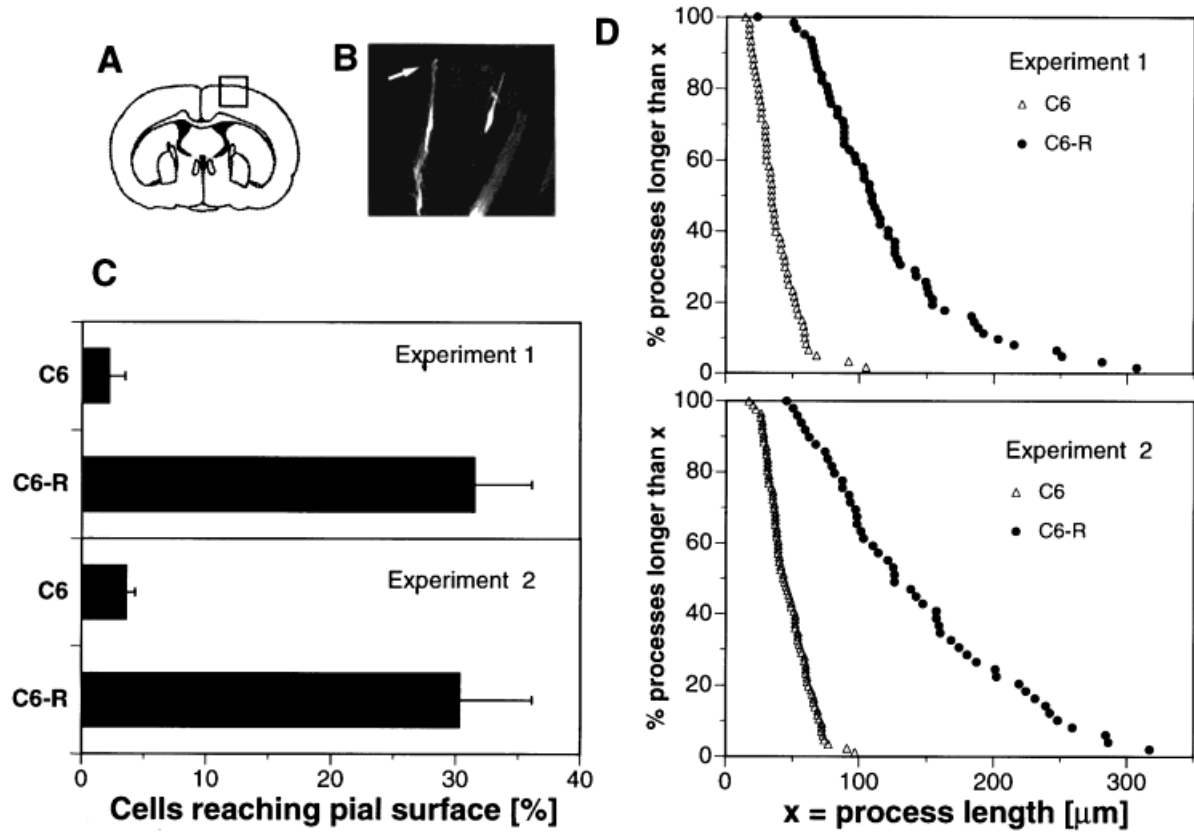
Figure 8 Analysis of pial contact and process length of C6-R and C6 cells. (A) Coronal section of an E19 rat brain illustrating the area used for quantification. (B) GFP-positive C6-R cells were injected at E16 and analyzed on E19 within the boxed area in (A). (C) Percentage of GFP-positive C6 and C6-R cells reaching the pial surface. Serial sections from three embryos from two different experiments were analyzed. The fraction of cells that had reached the pial surface or maintained pial attachments [arrow in (B)] were counted. (D) The length of each cell was determined through various focal planes and plotted as a function of the percentage $> x$.

While several key features of C6-R cells resemble endogenous radial glia, there are some differences. A peculiarity *in vivo* of the C6-R cells by comparison to radial glia is the position of their nuclei. Whereas the nuclei of radial glia are located near the ventricular surface, the nuclei of C6-R cells *in vivo* were not found to be restricted to this region. The polarity of nuclei in radial glia may relate to their patterns of cytokinesis near the ventricle. If C6-R cells divide *in vivo*, they may not do so at the ventricular surface, and this may affect the localization of their nuclei. In contrast to radial glia, C6-R cells proliferate rapidly in culture. However, their behavior in the brain suggests that they do not proliferate rapidly *in vivo*, which more closely resembles the behavior of radial glia *in vivo*.

The transplantation results with C6-R are particularly striking given that the parental C6 cell line is highly tumorigenic (Bernstein et al., 1990) but the C6-R cells are not (P. Brittis, A. Hormigo, D. Friedlander, B. Shif, D. Zagzag, and M. Grumet, unpublished observations). C6-R cells do not appear to form tumors in adult rat cortex, but they retain their radial phenotype in the adult brain for 1–2 weeks and then begin to disappear. This suggests that C6-R cells, like most radial glia, do not persist in the milieu of the adult rat brain cortex. Additional studies are needed to investigate the full potential of C6-R to differentiate in response to various cues that regulate the different types of cells that can originate from radial glia. It is possible that the ability of C6-R cells to respond to local cues *in vivo* may be an important factor that inhibits C6-R cells from forming tumors *in vivo*.

The molecular basis for the phenotype of C6-R, however, is not yet clear. C6 cells from which they were derived express two receptor forms of RPTPβ as well as a secreted form. The secreted form can act as an inhibitor of cell adhesion molecule-mediated glial

adhesion (Grumet et al., 1994; Sakurai et al., 1996) and neurite growth (Milev et al., 1994), and the short receptor form can promote neurite outgrowth by interacting with Nr-CAM and contactin on neurons (Sakurai et al., 1997), but the function of the receptor in glia is not understood. Indeed, the original goal of this project was to examine the role of RPTPβ by transfecting C6 glioma cells with a mutant form of this protein lacking the phosphatase domains. Through this approach we obtained the C6-R cell line as one of a few clones expressing relatively high levels of the mutant receptor. Since other cell lines expressing comparable or slightly lower levels of the mutant protein did not exhibit the dramatic polarized morphology of C6-R, it is likely that some other factor(s) must contribute to this phenotype. One possibility is that C6-R has a gain or loss of function resulting from integration of the transfection plasmid in a particular locus in the genome. Another possibility is that a mutation was generated in the C6 genome independent of the transfection. Preliminary Southern analysis indicates that plasmid integration occurred at a single locus which may help to identify a gene important for controlling the radial-like phenotype of C6-R.

The dramatic differences between C6 and C6-R in their morphological properties and behavior overshadow the molecular differences that have been detected so far. Nevertheless, quantitative differences have been detected for GFAP and RC1. The expression of these and other markers found in developing glia suggests that C6 glioma cells may represent a partially differentiated form of glia that has the potential for further differentiation. Indeed, treatment of C6 cells with cyclic adenosine monophosphate causes changes that have been interpreted as a form of astroglial differentiation in culture (Davies and Vernadakis, 1986). C6 cells appear to exhibit differentiation properties along different glial pathways (Perker et al., 1980), and the genetic alterations in C6-R may represent aspects of radial glial differentiation. Additional molecular studies are needed to compare C6-R with true radial glia.

In summary, the phenotype of C6-R and its ability to guide neuronal migration suggest that this cell line provides the first *in vitro* model for radial glia. Although other cell lines have been obtained that appear to be progenitors that can give rise to radial glia among other cells, their progeny are not homogenous in culture (McKay et al., 1990). Glial cells lines have also been obtained with a range of morphologies including radial-like cells, but they do not appear to

be as polarized as C6-R and have not been demonstrated to support neuronal migration or exhibit a radial glia phenotype *in vivo* (Alliot and Pessac, 1984). It is quite remarkable that a cell line with such highly polarized morphology could be obtained given the extensive cytoskeletal reorganization that occurs to complete cytokinesis. Moreover, C6-R can divide quite rapidly in culture, allowing one to obtain sufficient quantities for cell biological and biochemical experiments. Indeed, preliminary mRNA differential display studies indicate several differences between C6 and C6-R (A. Hormigo and M.Grumet, unpublished observations). Further cellular and molecular analysis of C6-R will reveal how closely this cell line resembles radial glia and may provide unique opportunities for studying key factors that control differentiation of these cells and their interactions with other neural cells during development. In that regard, C6-R may be particularly useful for studying receptors on radial glia such as the receptor for astrotactin.

REFERENCES

ALLIOT, F., and PESSAC, B. (1984). Astrocytic cell clones derived from established cultures of 8-day postnatal mouse cerebella. *Brain Res.* **306**:283–291.

ALVAREZ-BUYLLA, A., THEELEN, M., and NOTTEBOHM, F. (1990). Proliferation "hot spots" in adult avian ventricular zone reveal radial cell division. *Neuron* **5**:101–109.

ANTON, E. S., CAMERON, R. S., and RAKIC, P. (1996). Role of neuron-glial junctional domain proteins in the maintenance and termination of neuronal migration across the embryonic cerebral wall. *J. Neurosci.* **16**:2283–2293.

BERNSTEIN, J. J., GOLDBERG, W. J., LAWS, E. R., CONGER, D., MORREALE, V., and WOOD, L. R. (1990). C6 glioma cell invasion and migration of rat brain after neural homografting: ultrastructure. *Neurosurgery* **26**:622–628.

CANOLL, P. D., PETANCESKA, S., SCHLESSINGER, J., and MUSACCHIO, J. M. (1996). Three forms of RPTPβ are differentially expressed during gliogenesis in the developing rat brain and during glial cell differentiation in culture. *J. Neurosci. Res.* **44**:199–215.

CHALFIE, M., TU, Y., EUSKIRCHEN, G., WARD, W. W., and PRASHER, D. C. (1994). Green fluorescent protein as a marker for gene expression. *Science* **263**:802–805.

CULICAN, S. M., BAUMRIND, N. L., YAMAMOTO, M., and PEARLMAN, A. L. (1990). Cortical radial glia: identification in tissue culture and evidence for their transformation to astrocytes. *J. Neurosci.* **10**:684–692.

DAVIES, D. L., and VERNADAKIS, A. (1986). Responses in astrocytic C6 glioma cells to ethanol and dibutyryl cyclic AMP. *Brain Res.* **389**:253–260.

DIATCHENKO, L., LAU, Y.-F. C., CAMBELL, A. P., CHENCHIK, A., MOQDAM, F., HUANG, B., LUKYANOV, S., LUKYANOV, K., GURSKAYA, N., SVERDLOV, E. D., and SIEBERT, P. D. (1996). Suppression subtractive hybridization: a method for generating differentially regulated or tissue-specific cDNA probes and libraries. *Proc. Natl. Acad. Sci. USA* **93**:6025–6030.

EDMONDSON, J. C., and HATTEN, M. E. (1987). Glial-guided granule neuron migration in vitro: a high resolution time-lapse video microscopic study. *J. Neurosci.* **7**:1928–1934.

EDWARDS, M. A., YAMAMOTO, M., and CAVINESS, V. S. (1990). Organization of radial glia and related cells in the developing murine CNS: an analysis based upon a new monoclonal antibody marker. *Neuroscience* **36**:121–144.

FENG, L., and HEINTZ, N. (1995). Differentiating neurons activate transcription of the brain lipid-binding protein gene in radial glia through a novel regulatory element. *Development* **121**:1719–1730.

FISHELL, G. (1995). Striatal precursors adopt cortical identities in response to local cues. *Development* **121**:803–812.

FISHELL, G., and HATTEN, M. E. (1991). Astrotactin provides a receptor system for CNS neuronal migration. *Development* **113**:755–765.

FISHELL, G., and VAN DER KOOY, D. (1987). Pattern formation in the striatum: developmental changes in the distribution of striatonigral neurons. *J.Neurosci.* **7**:1969–1978.

FRIEDLANDER, D. R., MEGE, R.-M., CUNNINGHAM, B. A., and EDELMAN, G. M. (1989). Cell sorting-out is modulated by both the specificity and amount of different cell adhesion molecules (CAMs) expressed on cell surfaces. *Proc. Natl. Acad. Sci. USA* **86**:7043–7047.

FRIEDLANDER, D. R., ZAGZAG, D., SHIF, B., COHEN, H., ALLEN, J. C., KELLY, P. J., and GRUMET, M. (1996). Migration of brain tumor cells on extracellular matrix proteins in vitro correlates with tumor type and grade, and involves av and β1 integrins. *Cancer Res.* **56**:1939–1947.

GRAY, G. E., and SANES, J. R. (1992). Lineage of radial glia in the chicken optic tectum. *Development* **114**:271–283.

GRUMET, M., FRIEDLANDER, D. R., and SAKURAI, T. (1996). Functions of brain chondroitin sulfate proteoglycans during development: interactions with adhesion molecules. *Persp. Dev. Neurobiol.* **3**:319–330.

GRUMET, M., MILEV, P., SAKURAI, T., KARTHIKEYAN, L., BOURDON, M. A., MARGOLIS, R. K., and MARGOLIS, R. U. (1994). Interactions with tenascin and differential effects on cell adhesion of neurocan and phosphacan, two major chondroitin sulfate proteoglycans of nervous tissue. *J. Biol. Chem.* **269**:12142–12146.

HATTEN, M. E. (1985). Neuronal regulation of astroglial morphology and proliferation in vitro. *J. Cell Biol.* **100**:384–396.

HATTEN, M. E. (1993). The role of migration in central nervous system neuronal development. *Curr. Opin. Neurobiol.* **3**:38–44.

HOCKFIELD, S., and MCKAY, R. (1985). Identification of major cell classes in the developing mammalian nervous system. *J. Neurosci.* **5**:3310–3328.

HU, P., MONDINO, A., SKOLNIK, E. Y., and SCHLESSINGER, J. (1993). Cloning of a novel, ubiquitously expressed human phosphatidylinositol 3-kinase and identification of its binding site on p85. *Mol. Cell. Biol.* **13**:7677–7688.

HUNTER, K. E., and HATTEN, M. E. (1995). Radial glial cell transformation to astrocytes is bidirectional: regulation by a diffusible factor in embryonic forebrain. *Proc. Natl. Acad. Sci. USA* **92**:2061–2065.

JACOBSON, M. J. (1991). *Developmental Neurobiology*, 3rd ed. Plenum Press, New York.

LEVITT, P., COOPER, M. L., and RAKIC, P. (1983). Early divergence and changing proportions of neuronal and glial precursor cells in the primate cerebral ventricular zone. *Dev. Biol.* **96**:172–184.

LEVY, J. B., CANOLL, P. D., SILVENNOINEN, O., BARNEA, G., MORSE, B., HONEGGER, A. M., HUANG, J.-T., CANNIZZARO, L. A., PARK, S.-H., DRUCK, T., HUEBNER, K., SAP, J., EHRLICH, M., MUSACCHIO, J. M., and SCHLESSINGER, J. (1993). The cloning of a receptor-type protein tyrosine phosphatase expressed in the central nervous system. *J. Biol. Chem.* **268**:10573–10581.

LIANG, P., and PARDEE, A. B. (1992). Differential display of eukaryotic messenger RNA by means of the polymerase chain reaction. *Science* **257**:967–971.

MAUREL, P., RAUCH, U., FLAD, M., MARGOLIS, R. K., and MARGOLIS, R. U. (1994). Phosphacan, a chondroitin sulfate proteoglycan of brain that interacts with neurons and neural cell adhesion molecules, is an extracellular variant of a receptor-type protein tyrosine phosphatase. *Proc. Natl. Acad. Sci. USA* **91**:2512–2516.

MCKAY, R., VALTZ, N., CUNNINGHAM, M., and HAYES, T. (1990). Mechanisms regulating cell number and type in the mammalian central nervous system. *Cold Spring Harbor Symp. Quant. Biol.* **55**:291–301.

MILEV, P., FRIEDLANDER, D. R., SAKURAI, T., KARTHIKEYAN, L., FLAD, M., MARGOLIS, R. K., GRUMET, M., and MARGOLIS, R. U. (1994). Interactions of the chondroitin sulfate proteoglycan phosphacan, the extracellular domain of a receptor-type tyrosine phosphatase, with neurons, glia, and neural cell adhesion molecules. *J. Cell Biol.* **127**:1703–1715.

MISSON, J.-P., EDWARDS, M. A., YAMAMOTO, M., and CAVINESS, V. S. (1988). Mitotic cycling of radial glial cells of the fetal murine cerebral wall: a combined autoradiographic and immunohistochemical study. *Dev. Brain Res.* **38**:183–190.

PERKER, K. K., NORENBER, M. D., and VERNADAKIS, A. (1980). Transdifferentiation of C6 glial cells in culture. *Science* **280**:179–181.

RAKIC, P. (1990). Principles of neural cell migration. *Experientia* **46**:882–891.

RAMÓN Y CAJAL, S. (1995). *Histology of the Nervous System of Man and Vertebrates.* Oxford University Press, New York, 1955.

RIVAS, R. J., and HATTEN, M. E. (1995). Motility and cytoskeletal organization of migrating cerebellar granule neurons. *J. Neurosci.* **15**:981–989.

SAKURAI, T., FRIEDLANDER, D. R., and GRUMET, M. (1996). Expression of polypeptide variants of receptor protein tyrosine phosphatase β: the secreted form, phosphacan, increases dramatically during embryonic development and modulates glial cell behavior in vitro. *J. Neurosci. Res.* **43**:694–706.

SAKURAI, T., LUSTIG, M., NATIV, M., HEMPERLY, J. J., SCHLESSINGER, J., PELES, E., and GRUMET, M. (1997). Induction of neurite outgrowth through neuronal cell ad-

hesion molecules contactin and Nr-CAM by extracellular regions of glial receptor tyrosine phosphatase β. *J. Cell Biol.* **136**:907–918.

SORIANO, E., ALVARADO-MALLART, M., DUMESNIL, N., DEL RIO, J. A., and SOTELO, C. (1997). Cajal-Retzius cells regulate the radial glia phenotype in the adult and developing cerebellum and alter granule cells migration. *Neuron* **18**:563–577.

VOIGT, T. (1989). Development of glial cells in the cerebral wall of ferrets: direct tracing of their transformation from radial glia into astrocytes. *J. Comp. Neurol.* **289**:–74–88.

ZHENG, C., HEINTZ, N., and HATTEN, M. E. (1996). CNS gene encoding astrotactin which supports neuronal migration along glial fibers. *Science* **272**:417–419.